# LEGIBILITY NOTICE

A major purpose of the Technical Information Center is to provide the broadest dissemination possible of information contained in DOE's Research and Development Reports to business, industry, the academic community, and federal, state and local governments.

Although a small portion of this report is not reproducible, it is being made available to expedite the availability of information on the research discussed herein.

**LA-UR** -88-2008

Received ...
AUG ... 1988



LA-UR--88-2008

DE88 014429

TITLE: ANALYSIS OF SP-100 CRITICAL EXPERIMENTS

AUTHOR(S): J. L. Sapir and D. I. Brandon, N-12,
Los Alamos National Laboratory
P. J. Collins, ANL, Idaho Falls, ID
C. L. Cowan, GE-SNET, San Jose, CA
C. A. Porter and S. V. Andre, Westinghouse Electric Corp.,
Madison, PA

SUBMITTED TO: To be presented at the ANS Reactor Physics Meeting on
September 19-22, 1988, in Jackson Hole, Wyoming.



Los Alamos National Laboratory
Los Alamos, New Mexico 87545

# ANALYSIS OF SP-100 CRITICAL EXPERIMENTS

J. L. Sapir and D. I. Brandon
Los Alamos National Laboratory, Los Alamos, NM 87545
P. J. Collins
Argonne National Laboratory, Idaho Falls, ID 83403
C. L. Cowan
General Electric Company, San Jose, CA 95153
C. A. Porter and S. V. Andre'
Westinghouse Electric Corporation, Madison, PA 15663

## ABSTRACT

In support of the SP-100 space nuclear power source program, preliminary critical benchmark experiments were performed at the ZPPR facility at ANL-W. These configurations are representative of small, fast-spectrum, BeO-reflected, liquid metal-cooled space reactor designs at a 300-kWe power level. Analyses were performed using MCNP (Monte Carlo) and TWODANT (discrete ordinates) transport codes to calculate system criticality, control worth, and power distribution. Both methods calculated eigenvalues within 0.5% of the experimental results. Internal-poison-rod worth was underpredicted and radial reflector worth was overpredicted by both codes by up to 20%. MCNP-calculated control drum worths were underestimated by approximately 8%. Good agreement with experimental values was observed for $^{235}U$ fission and for $^{238}U$ fission and capture rates with the best agreement occurring in the fuel region and slightly poorer predictions apparent near BeO moderator.

## INTRODUCTION

To validate the nuclear power source for the SP-100 Reference Flight System (RFS), the Nuclear Assembly Test (NAT) is being designed and developed as part of a Ground Engineering System (GES) Program under the joint sponsorship of the United States Department of Energy, Department of Defense, and National Aeronautics and Space Administration. The objective of this program is to provide an electrical power source of 100 kWe to meet space mission requirements in the 1990s.

To support the design of the NAT, a series of critical experiments was performed in the fourth quarter of calendar year 1986 utilizing Assembly 16 of the Zero Power Physics Reactor (ZPPR-16) at Argonne National Laboratory-West. The critical experiments were carried out for representative SP-100 designs that were designed to supply a power of 300 kWe.[1,2] A goal of the criticals program was the establishment of experimental "benchmarks" to provide calibration factors (i. e., calculated-to-experimental (C/E) data points) for normalizing the key RFS nuclear performance parameters. Of particular interest was the generation of calibration factors for predicting the system criticality, control worth, and power distribution. Another goal of the criticals program was to provide criticality information relating to safety requirements for the flooding and loss of coolant accidents.

Experimental modeling of the RFS design in the ZPPR facility represented a major challenge because the reactor is a small, fast-spectrum, BeO-reflected system with enriched uranium nitride fuel pins, lithium coolant, and a niobium-based alloy for the cladding and structural materials. The development of an accurate experimental model of the small system was important to ensure that the characteristics of the high-leakage core were retained. Similarly, because of the limited material availability at the ZPPR facility, some care was required in the selection of the core constituents. In particular, judgement was required in the substitution of uranium metal, graphite, and sodium for the uranium nitride fuel and lithium coolant to ensure that the spectrum was adequately represented.

The analysis of the SP-100 critical experiments in ZPPR-16 was carried out as a cooperative effort among Argonne National Laboratory (ANL-W), Los Alamos National Laboratory (LANL), Westinghouse Advanced Energy Systems Division (WAESD), and the General Electric Company (GE). A description of the ZPPR-16 test program and results of selected analyses are presented in the sections that follow.

## ZPPR FACILITY

The ZPPR critical assembly machine is of the horizontal, split-table type consisting of a large, honeycomb array of square, stainless steel matrix tubes divided into separable halves. A photograph of the ZPPR assembly machine is shown in Figure 1 and a matrix-half containing the ZPPR-16A configuration is shown in Figure 2.

Stainless steel drawers, nominally 51-mm-square by 584- or 914- mm-long are inserted into the matrix tubes. The drawers are loaded with columns of rectangular plates or blocks used to simulate the fuel, structural, coolant, and control materials present in the reactor design. In some cases a calandria containing fuel or poison pins is loaded into a drawer. A photo of a typical plate-loaded drawer along with a pin-loaded calandria is shown in Figure 3. The final configuration is formed by bringing the loaded reactor halves together, and adjusting a fuel- or poison-bearing shim rod to achieve criticality.

Because of geometrical and material limitations, the ZPPR-16 critical assemblies differed from their corresponding SP-100 designs. Thus, rectangular plates were used to simulate a triangular fuel pin lattice. Heterogeneity effects associated with this geometrical difference are not expected to be significant in the fast-spectrum assembly.

Because uranium nitride was not available for the ZPPR-16 measurements, uranium metal and graphite were used to simulate the SP-100 fuel material. Enrichments of 93, 74, 56, and 37% were obtained by combining the appropriate number of highly enriched and depleted uranium fuel plates. Sodium was used in place of the unavailable lithium coolant, and the fuel pin liner material (currently rhenium) was omitted. The ZPPR matrix tubes and drawers contain a significant amount of stainless steel that will not be present in the SP-100 reactor. Where appropriate, this steel was used to offset some of the niobium present in the reactor (in the core, fission gas plenum, and pressure vessel regions). In other areas such as the radial reflector and the region outside the reactor, the steel constitutes an extraneous diluent. The limited inventory of niobium plates was used to simulate cladding in the central core region. The remainder of niobium in the reactor was mocked up with stainless steel plates. A schematic of a typical ZPPR-16B core drawer is shown in Figure 4. The front 6 inches of the drawer simulates a fuel lattice with 37%-enriched uranium, and the next 4 inches

Fig. 1 · ZPPR Assembly Machine

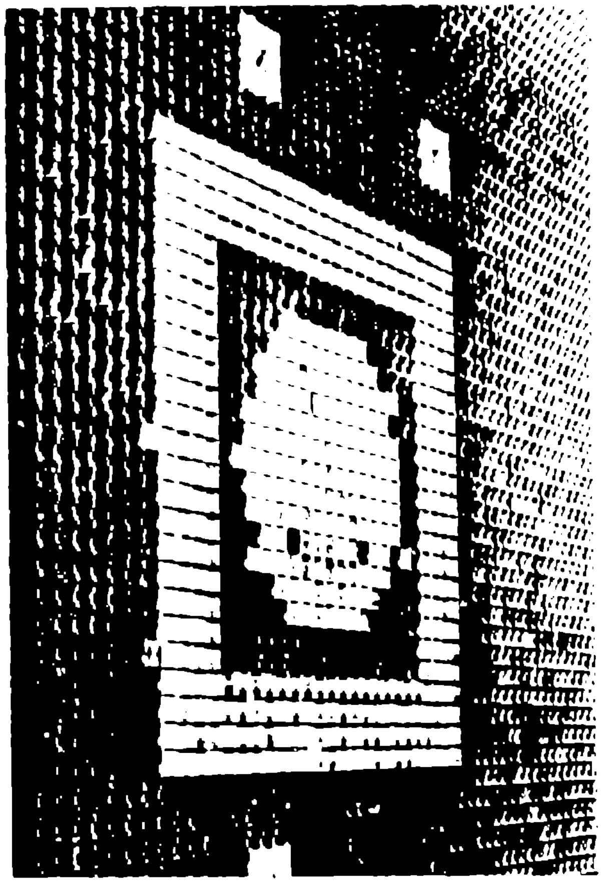

Fig. 2 · ZPPR-16A assembly loaded into matrix

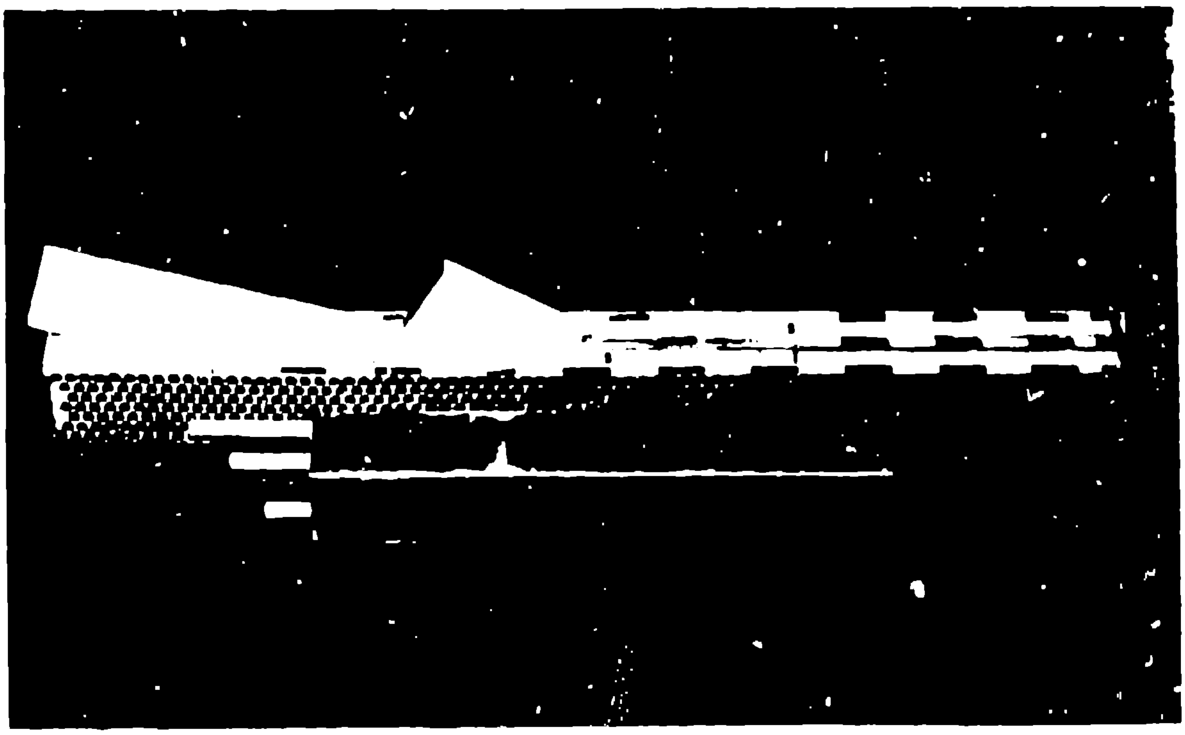

Fig. 3 · Typical ZPPR plate-loaded drawer and pin-loaded calandria

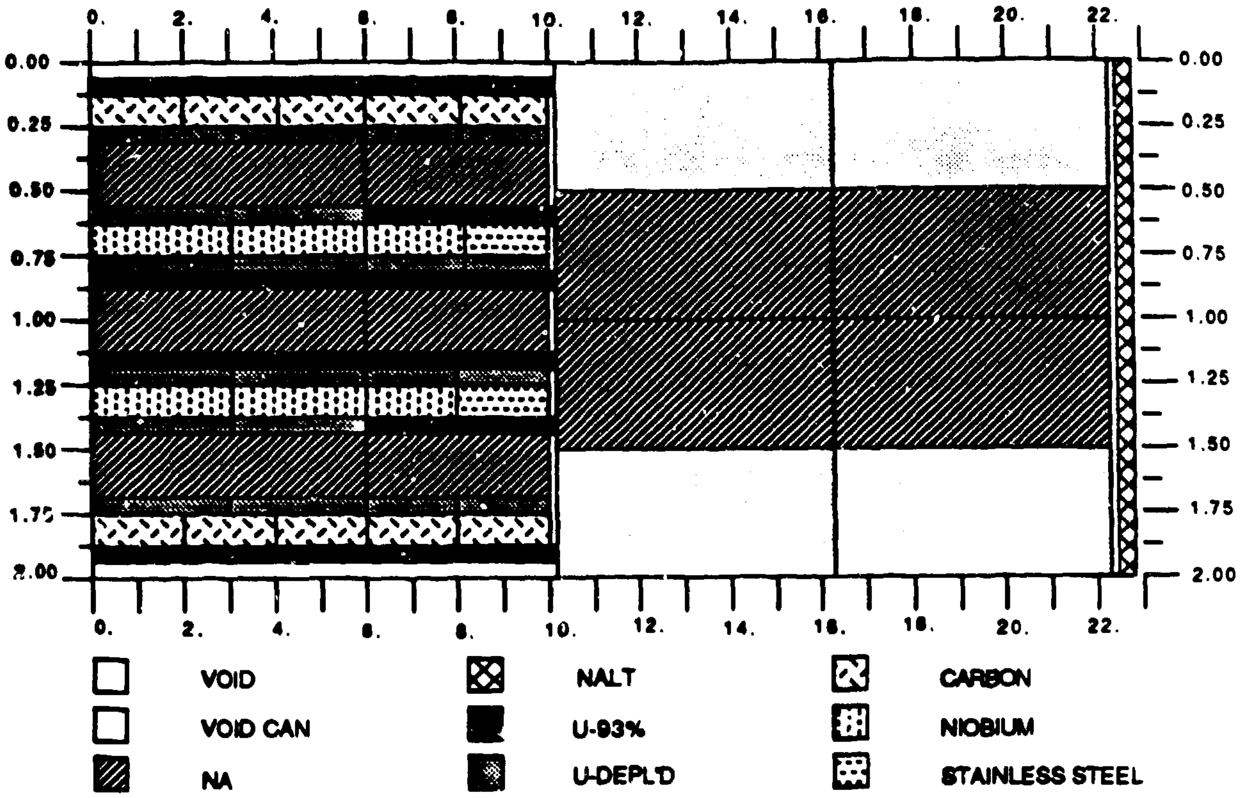


Fig. 4. Schematic of ZPPR-16B core drawer

simulates 56%-enriched fuel. The remainder of the drawer contains sodium and void cans representing the coolant plenum.

Although there were many differences between the ZPPR-16 critical mockups and the corresponding SP-100 designs, the mockups are very valuable experimental benchmarks to evaluate the accuracy of design methods and cross-section data in the areas of basic criticality, control worths, power distribution, and material replacement coefficients. Finally, it should be noted that the current SP-100 design is significantly different from the ones used to establish the ZPPR-16 assemblies, and a new critical-experiment program (ZPPR-20) to investigate the latest reactor design is currently underway.

## ZPPR-16 CONFIGURATIONS

Two core designs were modeled in the ZPPR-16 experiments. ZPPR-16A was based on a LANL design which had thirteen internal control rod positions (CRPs) and a thin beryllium oxide radial reflector. A schematic of ZPPR-16A is shown in Figure 5. In the critical configuration the central and six outer poison rods were fully inserted while the middle six positions contained BeO followers. The active core was 62-cm-long, effectively 47 cm in diameter, and contained fuel enrichments zones of 56, 74, and 93%. A 1.4-cm-thick stainless steel pressure vessel followed by a 4-cm-thick BeO reflector surrounded the core in the radial direction. No axial reflector was present, but axial coolant and fission gas plena were simulated with sodium, stainless steel, and void.

ZPPR-16B was based on a GE design[2] with six internal safety rods and a relatively thick (8.7 cm) BeO radial reflector that incorporated twelve rotating $B_4C$/BeO control drums. In the critical configuration the six internal CRPs

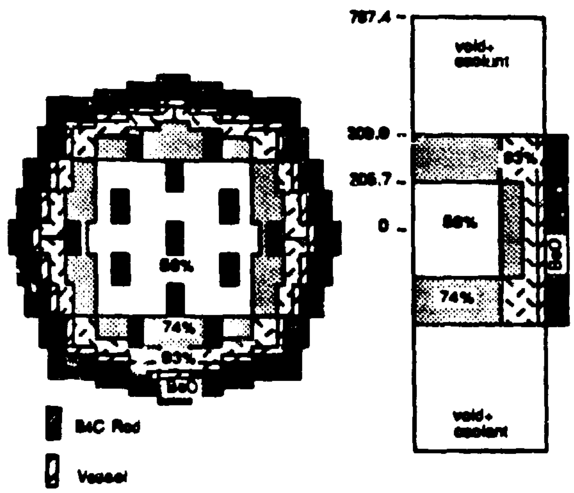


Fig. 5 ZPPR-16A Interface and Axial Enrichment Zones

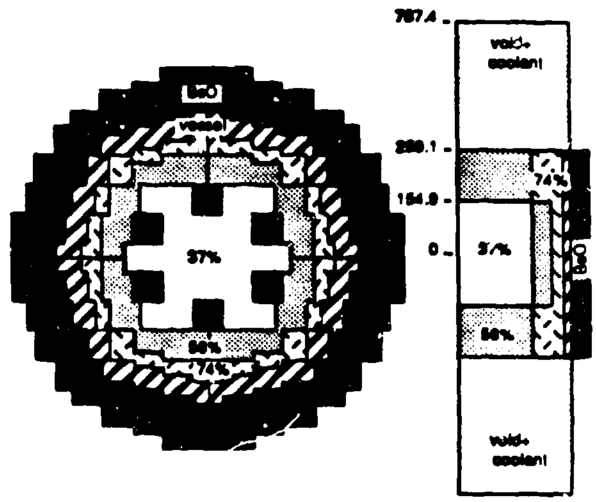


Fig. 6 ZPPR-16B Interface and Axial Enrichment Zones

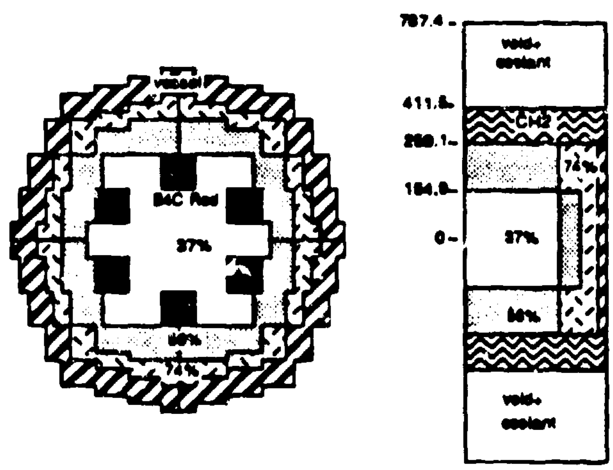


Fig. 7 ZPPR-16C Interface and Axial Enrichment Zones

contained BeO followers. To maintain a calculable, benchmark assembly, the basic 16B loading did not simulate the poison drums, but incorporated a "clean" radial reflector. Several experiments were, however, performed to estimate the effects of the drums. (The current GE design no longer includes rotating drums, but instead incorporates reflector motion with no internal poison to produce the required reactivity changes.) To compensate for the thicker BeO reflector and the absence of internal poison rods, the ZPPR-16B core enrichment zones were reduced to 37, 56, and 74%, and the active height was shortened to 52 cm. A schematic view of the 16B assembly is shown in Figure 6.

ZPPR-16C investigated a shutdown, water-flooded accident scenario. The core dimensions, fuel loadings, and structural materials were essentially the same as in 16B. The six BeO followers were replaced with enriched $B_4C$ safety rods, the sodium coolant and void in the core and axial plena were replaced with polyethylene, and the radial BeO reflector was removed. A schematic of the ZPPR-16C configuration is shown in Figure 7.

All phases included axial tungsten gamma-ray shields (787 mm from the core midplane), and axial and radial shields of $B_4C$ and graphite (borated polyethylene in the lower axial region) to reduce the effect of room-return neutrons and provide a manageable boundary for the analyses. It turned out that the radial shield had a significant reactivity effect, increasing $k_{eff}$ by about 4%.

## EXPERIMENTAL PROGRAM

The ZPPR-16 experimental program is summarized in Table I. Critical loadings were determined for all phases. The ratio of the effective delayed neutron fraction to the prompt neutron lifetime was measured by noise coherence in 16A and 16B. Control worth measurements included the determination of the internal-poison-rod-bank and radial reflector worths in 16A and 16B. Several experiments were also performed in 16B to estimate control drum worths. Detailed power distributions were measured with $^{235}U$ and $^{238}U$ foils, gamma-dose distributions were measured with thermoluminescent detectors, and neutron spectra were measured using proton recoil counters. Material worth measurements, using an oscillator, were made in 16B and 16C.

TABLE I. ZPPR-16 Experimental Program

| Parameter | 16A | 16B | 16C |
|---|---|---|---|
| Criticality | X | X | X |
| Kinetics | X | X | X |
| Control Rod Worths | X | X | |
| Reflector Worths | X | X | |
| Power Distribution | X | X | |
| Gamma Ray Dose Distribution | X | X | |
| Neutron Spectrum | X | X | |
| Material Worths | | X | X |

## ANALYSES

Calculations were performed for the ZPPR-16 configurations by personnel at ANL-W, Westinghouse, and Los Alamos. The primary purposes of the ANL-W calculations were to aid in the design of the experiments, and to provide quantities required for processing experimental data. Westinghouse performed an extensive series of detailed calculations to establish preliminary calibration factors for SP-100 core design activities. Los Alamos provided calculational support in both the planning and analysis areas.

Of the two normal operational configurations investigated, the 16B assembly more closely resembles the evolving SP-100 reactor design. The control location and reflector thickness are more representative, although the fuel enrichment is less than current levels. Furthermore, the water-flooded configuration, an important safety concern, was only established for the 16B design. Therefore, the calculations and analyses described in this paper will focus on the 16B and 16C configurations. We will also stress those calculations used to establish the SP-100 calibration factors. More detailed and comprehensive reports describing methods and results will be published by ANL-W and Westinghouse.

### Methodology

Figure 8 shows a schematic flow diagram depicting several of the calculational methods used in the analyses. Basic cross-section data were obtained from the ENDF/B-V.2 data base. Several codes including NJOY and TRANSX were used to process the basic cross-section data into the formats required by the reactor techniques, namely Monte Carlo and discrete ordinates ($S_n$) transport-theory.

The NJOY code[3] produces a library of continuous-energy cross sections for use directly by the Monte Carlo code, or multigroup libraries that are further processed by TRANSX[4] into a format compatible for use in the discrete ordinates codes. The TRANSX code was used in conjunction with the NJOY-generated MATXS6 library which contains data for 80 neutron groups and 24 gamma groups. TRANSX options include resonance self-shielding, Doppler-broadening, transport and elastic removal corrections, spatial flux-weighting, and group collapse. Several multigroup libraries were prepared including an 80 and a 30 neutron-group set, as well as a coupled library with 11 neutron and 4 photon groups.

Because diffusion theory was expected to give less accurate results than transport theory for the small, leakage-dependent, beryllium-reflected system, transport techniques were selected as the principle analytical approach. A few diffusion calculations performed early in the program yielded $k_{eff}$ values approximately 6% lower than the corresponding transport theory results.

The $S_n$ calculations were performed with the one-dimensional ONEDANT[5] and two-dimensional TWODANT[6] codes that numerically solve the multigroup form of the Boltzmann transport equation using the discrete ordinates approximation to treat angular flux variations. Most calculations were run with $S_4$ segmentation and $P_1$ scattering, with several comparison checks made with higher order approximations.

Monte Carlo analysis was performed with the MCNP code.[7] MCNP is a general-purpose, continuous-energy, generalized-geometry, time-dependent, coupled neutron-photon Monte Carlo transport code. It includes the capability to

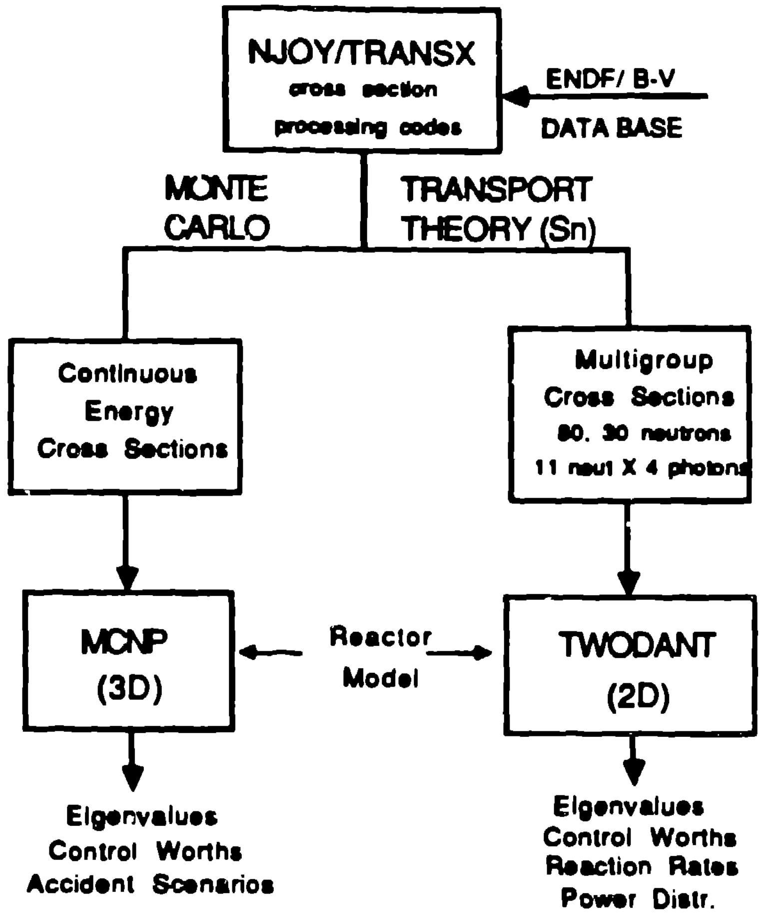


Fig. 8 Representative Calculational Methods

calculate eigenvalues for multiplying systems, and allows a very detailed and accurate geometrical representation of the reactor design or experimental configuration.

## Eigenvalue Calculations

The TWODANT calculational model for ZPPR-16B was derived from basic drawer masters and ADEN (plate-mass) data furnished by ANL-W. The ZPPR x,y,z geometry was converted to a r,z model by conserving material masses and cylindricizing areas in the radial direction. Drawers and partial drawers were grouped into radial zones to preserve discrete regions such as enrichment zones, pressure vessel, and reflector. The resulting r,z calculational model is shown, schematically in Figure 9. To reduce computational time, the model assumes axial symmetry about the core midplane. Regions 38 thru 49 in the model are an average composite of the actual upper and lower axial shield regions. Separate mixture cross sections were prepared for each of the zones shown in Figure 9. These cross sections were $P_1$, transport-corrected, and contained 80 neutron energy groups. The calculated value of $k_{eff}$ for the r,z model was 1.0050.

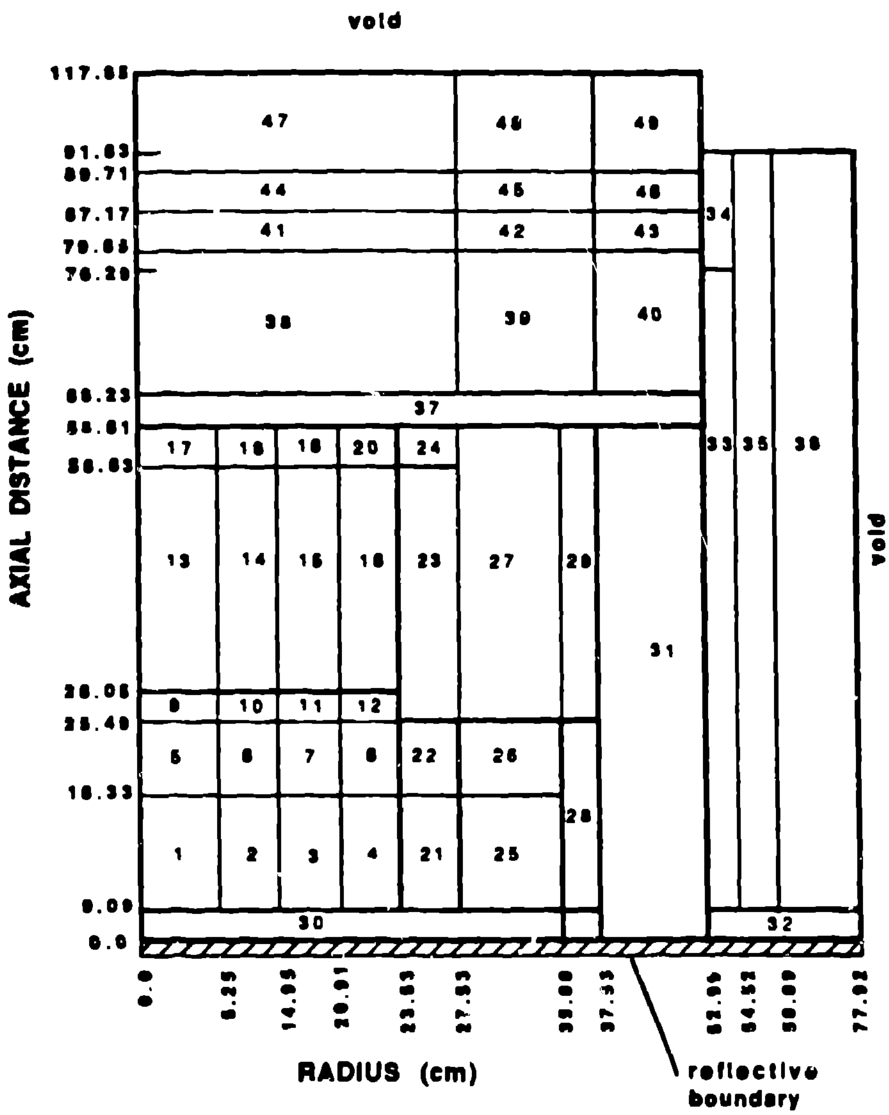


1 Fuel, 37% enriched
2 37% enriched + BeO
3 Fuel, 56% enriched
4 Fuel, 74% enriched
5 Fuel, 56% enriched
6 56% enriched + BeO
7 Fuel, 74% enriched
8 Fuel, 74% enriched
9 Fuel end
10 Fuel end
11 Fuel end
12 Fuel end
13 Plenum
14 Plenum
15 Plenum
16 Plenum
17 Drawer end
18 Drawer end
19 Drawer end
20 Drawer end
21 Pressure vessel
22 Pressure vessel
23 Void cans
24 Drawer end
25 Reflector
26 Reflector
27 Void cans
28 Void cans
29 Empty drawers
30 23" front plate
31 Empty Matrix
32 36" front plate
33 Radial shield, B4C
34 Radial shield, B4C
35 Radial shield, void
36 Radial shield, graphite
37 Drawer hardware
38 Axial shield.
39 Axial shield
40 Axial shield
41 Axial shield, tungsten
42 Axial shield, tungsten
43 Axial shield, tungsten
44 Axial shield, B-Poly
45 Axial shield, B-Poly
46 Axial shield, B-Poly
47 Axial shield, poly
48 Axial shield, poly
49 Axial shield, graphite

Fig. 9 r,z Calculational Model

Construction of the r,z model requires conversion from the actual x,y geometry of the ZPPR matrix into an equivalent cylindrical geometry, and the "smearing " of control rod drawers into annuli. To evaluate potential biases associated with these approximations we compared the results of equivalent TWODANT x,y and ONEDANT r,z calculations. The resulting $k_{eff}$ differences were -0.002 for the x,y to r,z conversion, and essentially zero for the homogenization of the BeO drawers. Homogenizing $B_4C$ poison rods would, however, be significant.

The results of the $S_n$ eigenvalue calculations are summarized in Table II. Applying the corrections to the calculated r,z $k_{eff}$ of 1.0050 yields a corrected eigenvalue of 1.003, in very good agreement with the experimental result. We did not calculate the effects of local heterogeneities on the predicted eigenvalue. Early estimates indicated these effects would be small in the non-flooded cells, about +0.4% $\Delta k$, and partially compensated by streaming effects of similar magnitude, -0.2% $\Delta k$. Larger heterogeneity effects of 2-3% $\Delta k$ are expected in the flooded cells.

A detailed three-dimensional model of ZPPR-16B was created for MCNP calculations. Because of computer memory constraints, the model was limited to a one-eigth-core-section (upper right-hand quadrant in Half 1) with the application of appropriate reflective boundary conditions. The only notable assymmetries associated with this approximation are small geometric and material perturbations due to instrumentation (not considered significant) and different axial shields in Half 1 and Half 2. Sensitivity calculations indicated that the axial shield effect would require a correction of -0.002 $\Delta k$ to the Half 1 results. Because this correction is less than the statistical uncertainty in the eigenvalue calculation (typically ±0.004), no adjustments to the Half 1 results were made.

The MCNP calculations modeled each plate in every drawer explicitly. Contiguous identical plates were defined as a single cell whenever possible. Within-cell gaps and/or void space were explicitly represented. The matrix and drawer structure were combined to form cells that surrounded the drawer contents. Approximately 1900 cells were required to specify the reactor and 240 planes to define the cell boundaries.

The ZPPR-16C calculational model was a direct extension of the 16B model. The calandria and poison pins were explicitly modeled replacing the BeO followers. Similarly, polyethylene plates were substituted for void and sodium-filled cans, and the BeO reflector drawers were removed.

The MCNP eigenvalue results and the corresponding C/E ratios are shown in Table II. Agreement between calculations and experiments are within 0.005 $\Delta k$ for both the 16B and 16C configurations.

## Control Worths

A series of subcritical multiplication measurements were performed in ZPPR-16B to investigate various control techniques. These measurements included insertion of the six internal poison rods, complete removal of the radial reflector, and simulation of rotating poison control drums in the radial reflector.

Table II - CALCULATIONAL RESULTS

| | Exp'l. | TWODANT | | MCNP | |
|---|---|---|---|---|---|
| | Value | Value | C/E | Value | C/E |
| EIGENVALUE | | | | | |
| ZPPR-16B | 1.002 | 1.003 | 1.002 | 1.005±0.4% | 1.004 |
| ZPPR-16C | 1.002 | - | - | 1.007±0.4% | 1.005 |
| CONTROL WORTH ($) | | | | | |
| Internal rods | 27.8 | 23.9† | 0.86 | 22.6±3.4%† | 0.81 |
| Radial reflector | 20.3 | 24.4† | 1.20 | 22.6±3.4%† | 1.11 |
| Drums in/no gaps | 11.6 | - | - | 10.8±8.4%† | 0.92 |
| Drums in/with gaps | 12.8 | - | - | 11.7±7.6%† | 0.92 |

† $(k_1 - k_2) / k_1 * k_2 * \beta_{eff}$
where calculated value of $\beta_{eff}$ = 0.00725

The control worth calculations used the same codes, procedures and models previously described for the eigenvalue calculations, with the control system positions altered to model the experimental configurations. A $\beta_{eff}$ value of 0.00725, determined from a TWODANT-based perturbation calculation, was used to convert the calculated $\Delta k$ values to units of dollars. The calculated control worths and corresponding C/E ratios are summarized in Table II for both TWODANT and MCNP calculations. In the case of internal-rod insertion and reflector removal, the TWODANT and MCNP results are consistent, but significantly different from the experimental values, with the calculations underpredicting the internal-rod worth, and overestimating the reflector worth. The calculated control drum worths are approximately 8% less than the corresponding measured values.

**Reaction Rates**

Isotopic neutron fission and capture rates were measured in ZPPR-16 to provide experimental verification of the SP-100 design methods and cross-section data related to power distribution parameters. The experiments consisted of foil activation measurements of $^{235}U$ fission rates, $^{238}U$ fission and capture rates, and thermoluminescent dosimeter (TLD) measurements of gamma heating rates. Reaction-rate measurements were performed in a large number of locations throughout the symmetric quadrant of the ZPPR-16B assembly near the core midplane. Axial distributions were also measured in selected fuel drawers.

The power distribution analyses were performed with the TWODANT code in x,y and r,z geometries. A utility code was used to interpolate the calculated flux data to the exact measurement locations. The calculated reaction rates were normalized such that the average calculated $^{235}U$ fission rate in the fuel was set equal to the average measured value.

The calculated C/E ratios for the radial $^{235}U$ fission distribution are shown in Figure 10. Good agreement (within 5%) is observed in the fuel region, although poorer predictions are apparent in the vicinity of the BeO moderator (both near

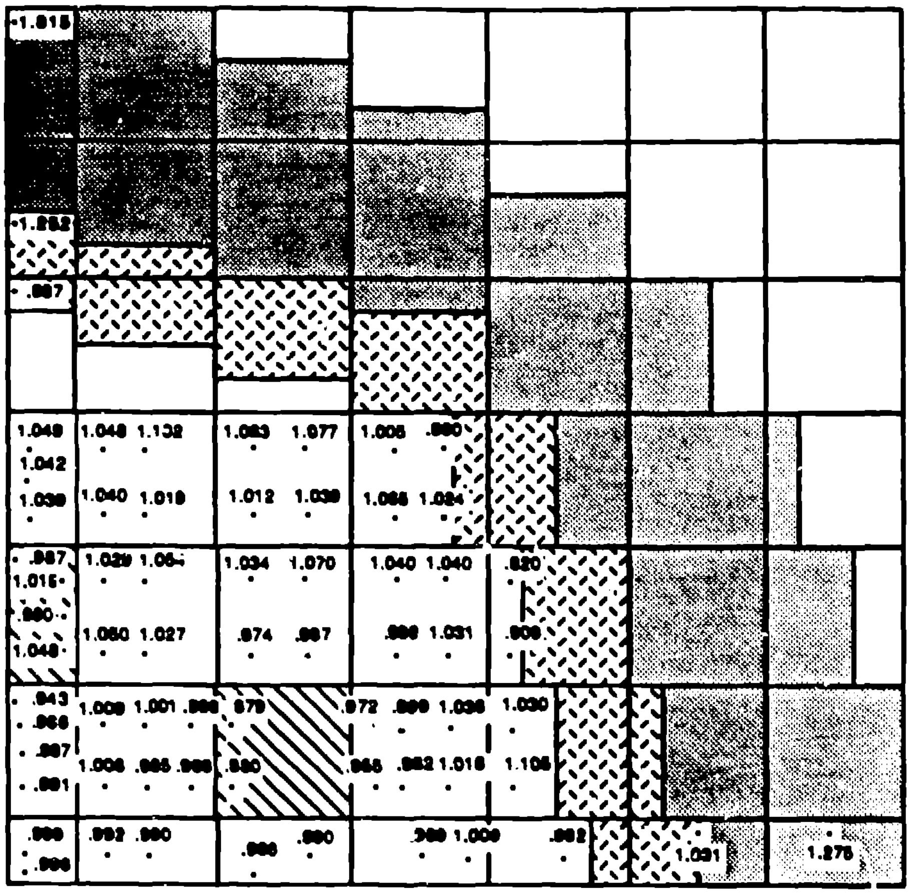

Fig. 10 Comparison of measured and calculated $^{235}U$ fission rates (16 mesh per drawer).

internal-rod followers and at the core periphery). The effects of higher-order approximations (64 vs 16 mesh per drawer, and $S_{16}$ vs $S_8$ quadrature) on the calculated fission distribution were investigated. Increasing the mesh intervals yielded notably better agreement at the core periphery, while the improvement due to higher quadrature was very slight, and judged not worth the additional computational costs.

Calculated and measured radial and axial $^{235}U$ fission-rate distributions are compared in Figures 11 and 12, respectively. In general, very good agreement exists in the fuel regions away from beryllium, suggesting that the fast neutron flux is accurately calculated. Larger differences although still in reasonable agreement) appear in core regions close to beryllium, implying slight mispredictions associated with beryllium moderation. In regions outside the core (beyond the vessel) the differences increase. The use of a finer mesh structure and variable axial bucklings should reduce these differences.

Calculated $^{238}U$ fission rates agreed closely with experimental values throughout both the core *and* reflector, confirming the accuracy of the fast flux calulations. The calculated $^{238}U$ capture rates more closely resembled the $^{235}U$ results, exhibiting relatively large discrpancies outside the core. After normalizing the calculated fluxes to agree with the average $^{235}U$ core fissions, the calculated $^{238}U$ fission rates averaged approximately 4% more than the measured values.

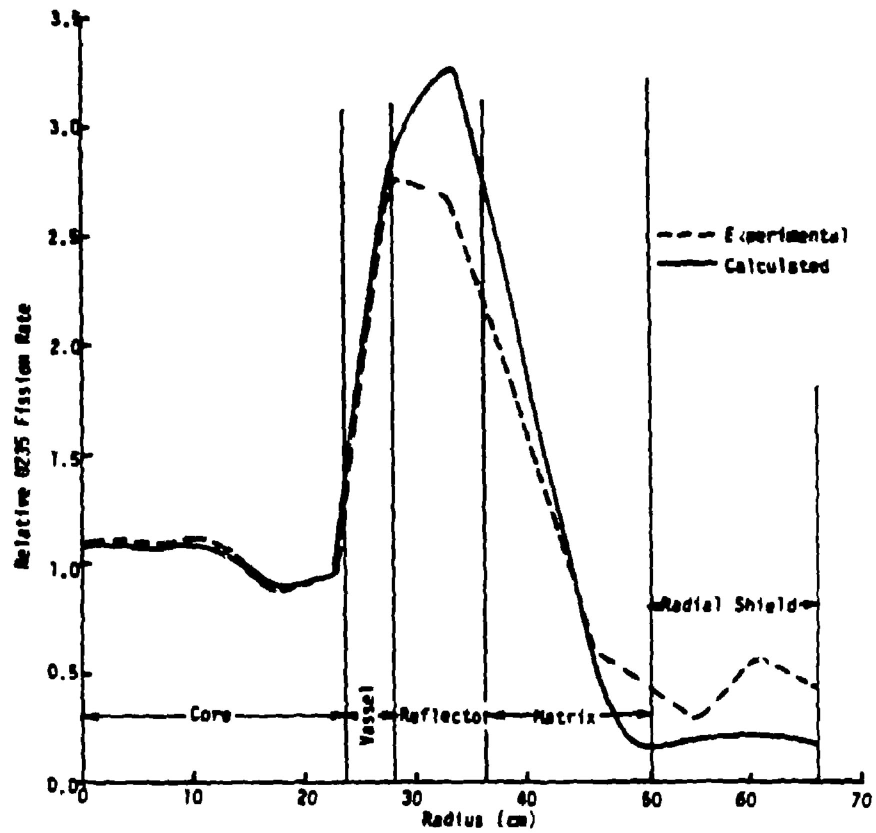


Fig. 11 Radial $^{235}U$ fission rate comparison

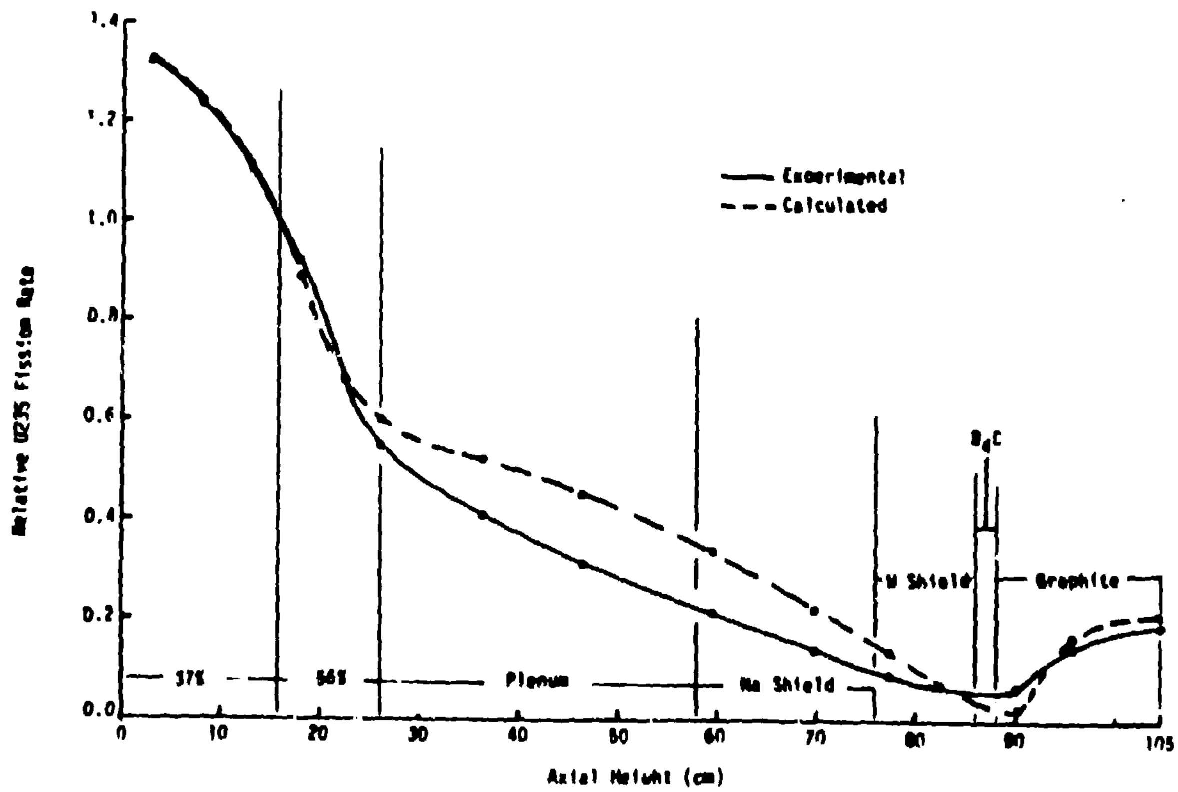


Fig. 12 Axial fission rate comparison for $^{235}U$ in central fuel drawer

## CONCLUSIONS

These results summarize the work that has been performed for the ZPPR-16 critical experiments in support of the SP-100 design effort. Because of the smaller active core volume, the analyses utilized transport computational techniques rather than diffusion methods predominantly employed in earlier liquid metal reactor design programs. Therefore, the ZPPR-16 experiments constitute an important early test of the accuracy of the selected SP-100 nuclear design codes and data. The comparison of measured and calculated quantities confirms the adequacy of these methods and provides preliminary calibration factors that quantify the magnitude of calculational biases. The ZPPR-16 critical measurements and associated calibration data provide a strong basis for the SP-100 core design calculations. A more comprehensive analysis of ZPPR-20 (SP-100 engineering mockup critical) will extend and refine the relevant data to ensure accurate, well predicted SP-100 performance characteristics.

## ACKNOWLEDGMENTS

The experiments were conducted by D.N. Olsen with assistance from the ZPPR staff. Detailed descriptions of the reactor loadings were provided by D. R. Tate from the ZPPR data base system. Numerous calculations required for processing experimental data were made by D. M. Smith and G. L. Grasseschi. S. G. Carpenter provided guidance throughout all phases of the ZPPR-16 program.

## REFERENCES

1. J. Sapir, R. Baars, D. Brandon, K. Cooper, J. Durkee, and M. Morgan, "Conceptual Design of a Reactor for a 300-kWe Space Nuclear Power System," Trans. 4th Symposium on Space Nuclear Power Systems, CONF-87102, Albuquerque, NM, January 12-16, 1987.

2. S. Vaidyanathan, S. Kaplan, R. Protsik, and A. Dalcher, "Design Concepts for the GES SP-100 Reactor and Shield, Trans. 4th Symposium on Space Nuclear Power Systems, CONF-87102, Albuquerque, NM, January 12-16, 1987.

3. R. E. MacFarlane, R. D. Barrett, D. W. Muir, and R. M. Boicourt, "The NJOY Nuclear Data Processing System: User's Manual," Los Alamos Scientific Laboratory report LA-7584-M (December 1978).

4. R. E. MacFarlane, "TRANSX-CTR: A Code for Interfacing MATXS Cross-Section Libraries to Nuclear Transport Codes for Fusion Systems Analysis," Los Alamos National Laboratory report LA-9863-MS (February 1984).

5. R. D. O'Dell, F. W. Brinkley, and D. R. Marr, "A User's Manual for ONEDANT: A Code Package for One-Dimensional, Diffusion-Accelerated, Neutral-Particle Transport," Los Alamos National Laboratory report LA-9184-M (February 1982).

6. R. E. Alcouffe, F. W. Brinkley, D. R. Marr, and R. D. O'Dell, "User's Guide for TWODANT: A Code Package for the Two-Dimensional, Diffusion-Accelerated, Neutral-Particle Transport," Los Alamos National Laboratory report LA-10049-M (March 1984).

7. J. F. Briesmeister, editor, "MCNP-A General Monte Carlo Code for Neutron and Photon Transport, Version 3A," Los Alamos National Laboratory report LA-7396-M, Rev. 2 (September 1986).